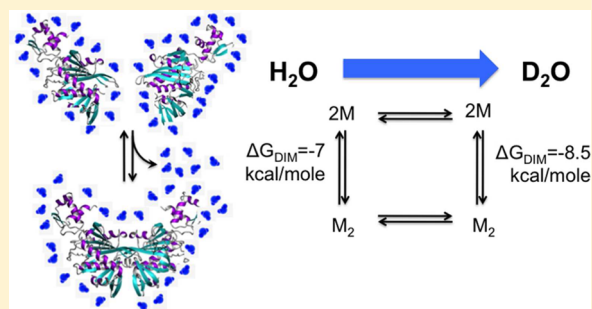


A Large Solvent Isotope Effect on Protein Association Thermodynamics

Christopher Eginton and Dorothy Beckett*

Department of Chemistry and Biochemistry, College of Computer, Mathematical and Natural Sciences, University of Maryland, College Park, Maryland 20742, United States

ABSTRACT: Solvent reorganization can contribute significantly to the energetics of protein–protein interactions. However, our knowledge of the magnitude of the energetic contribution is limited, in part, by a dearth of quantitative experimental measurements. The biotin repressor forms a homodimer as a prerequisite to DNA binding to repress transcription initiation. At 20 °C, the dimerization reaction, which is thermodynamically coupled to binding of a small ligand, bio-5'-AMP, is characterized by a Gibbs free energy of -7 kcal/mol. This modest net dimerization free energy reflects underlying, very large opposing enthalpic and entropic driving forces of 41 ± 3 and -48 ± 3 kcal/mol, respectively. The thermodynamics have been interpreted as indicating coupling of solvent release to dimerization. In this work, this interpretation has been investigated by measuring the effect of replacing H₂O with D₂O on the dimerization thermodynamics. Sedimentation equilibrium measurements performed at 20 °C reveal a solvent isotope effect of -1.5 kcal/mol on the Gibbs free energy of dimerization. Analysis of the temperature dependence of the reaction in D₂O indicates enthalpic and entropic contributions of 28 and -37 kcal/mol, respectively, considerably smaller than the values measured in H₂O. These large solvent isotope perturbations to the thermodynamics are consistent with a significant contribution of solvent release to the dimerization reaction.



Protein–protein interactions are central to a broad range of biological processes, including signal transduction,¹ transcription regulation,² and morphogenesis.³ Although the intrinsic chemistry of the interacting protein partners is important in determining the strength of an interaction, water, either through its release into the bulk upon interface formation or through its direct participation in the interface, is also integral to protein–protein interactions. Moreover, simulations predict that the interplay of protein sequence with solvent profoundly influences protein assembly reactions.⁴ Despite the widespread appreciation of its significance, experimental determination and computational prediction of the energetic contribution of solvent reorganization remain a challenge for understanding both the physical chemistry of protein–protein interactions and the design of novel interactions.⁵

Escherichia coli protein BirA forms a homodimer prior to binding to DNA to regulate transcription initiation.⁶ The dimerization reaction is thermodynamically coupled to small molecule bio-5'-AMP binding, which renders the protein–protein interaction more favorable by -4 kcal/mol (Figure 1).^{7,8} The equilibrium dimerization constant for bio-5'-AMP-bound BirA, holoBirA, is $6 \mu\text{M}$ at 20 °C, 200 mM KCl, and pH 7.5, which corresponds to a modest Gibbs free energy of -7 kcal/mol.⁸ By contrast, van't Hoff analysis of the temperature dependence of the reaction indicates very large opposing enthalpic ($\Delta H^\circ_{\text{DIM}}$) and entropic ($-T\Delta S^\circ_{\text{DIM}}$) driving forces of 41 and -48 kcal/mol, respectively, at 20 °C.⁹ Furthermore, the

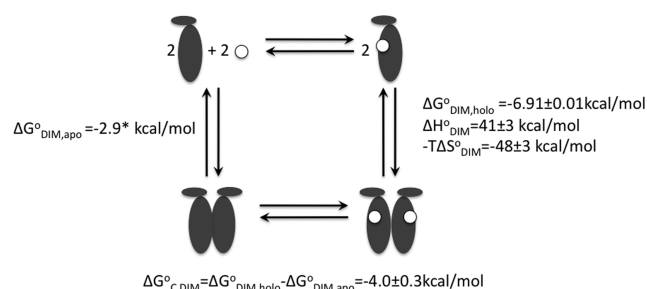


Figure 1. Thermodynamic cycle illustrating the linkage between BirA dimerization and bio-5'-AMP binding. The coupling ($\Delta G^\circ_{\text{C,DIM}}$) is calculated from the difference in the measured dimerization free energy of bio-5'-AMP-bound or holoBirA, and unliganded or apoBirA ($\Delta G^\circ_{\text{DIM,holo}} - \Delta G^\circ_{\text{DIM,apo}}$). The thermodynamic parameters for holoBirA dimerization are shown at the right: (white circle) bio-5'-AMP and (gray shape) BirA. The free energy of apoBirA dimerization in 200 mM KCl is calculated from the value measured in 50 mM KCl and the measured effect of salt concentration on holoBirA dimerization.^{8,9}

linearity of the van't Hoff plot obtained from analysis of the temperature dependence of the dimerization reaction is

Received: July 17, 2013

Revised: August 27, 2013

Published: August 28, 2013

consistent with the absence of a heat capacity change in the reaction.

The large opposing enthalpies and entropies of holoBirA dimerization are consistent with solvent release upon dimer formation.^{9,10} The enthalpic penalty may reflect the cost of removal of water from the dimerization surface concomitant with formation of the interface.¹¹ Likewise, the favorable entropy is consistent with the release of bound water to the bulk upon dimerization. The chemistry of the dimerization surface, which contains a number of polar and charged groups, is consistent with a large enthalpic penalty of removing surface-bound water during the course of dimerization.¹² Analysis of the dimer interface, in which 40% of the buried groups are polar, indicates the presence of 16 hydrogen bonds and four salt bridges.^{13,14} Furthermore, few water molecules are located in the interface. However, given the net unfavorable dimerization enthalpy is 41 kcal/mol, this structural interpretation of the thermodynamics assumes a desolvation penalty that is much larger than the favorable enthalpy associated with formation of combined intersolvent hydrogen and protein–protein interface bonds.

A number of experimental approaches have been used to investigate the contribution of water reorganization to biomolecular interactions. Addition of osmolytes allows measurements of the dependence of the reaction on water activity, thus providing information about the number of waters released or taken up in the course of binding. However, a potential complication to interpretation of the results lies in the preferential interaction of the osmolyte with one or more of the interacting partners.¹⁵ The volume change obtained from measuring the response of the equilibrium constant for an interaction to changes in hydrostatic pressure can be interpreted in terms of the linkage of water binding or release to the equilibrium process.¹⁶ Pressure perturbation calorimetry also provides a means of estimating the role of water reorganization in biomolecular interactions.¹⁷ Finally, because of the distinct hydrogen bonding properties of the two, measurements of the solvent isotope effect of replacing H₂O with D₂O have been used to estimate the contribution of water reorganization to protein–protein association.¹⁸

In this work, the role of solvent reorganization in holoBirA dimerization has been probed by measuring the consequences for the reaction of replacing H₂O with D₂O. Sedimentation equilibrium measurements performed on the wild-type and single-amino acid variants of BirA reveal that dimerization is consistently more favorable by approximately −1.5 kcal/mol in D₂O than in H₂O. van't Hoff analysis of the temperature dependence of the dimerization equilibrium measured in heavy water indicates linear behavior that yields an unfavorable dimerization enthalpy of 28 kcal/mol, 13 kcal/mol lower than that measured in H₂O. This enthalpy decrease is accompanied by a similarly large decrease in the favorable dimerization entropy. The results are consistent with a contribution of solvent reorganization to the holoBirA dimerization energetics.

MATERIALS AND METHODS

Chemicals and Biochemicals. All chemicals used in buffer preparation were at least reagent grade. The bio-S'-AMP was synthesized and purified as previously described.^{19,20} The standard buffer (10 mM Tris HCl, 200 mM KCl, and 2.5 mM MgCl₂) prepared in D₂O was adjusted to a pD of 7.5 using a meter reading of 7.1 to correct for the effect of deuterium on glass electrodes.²¹

Protein Preparation. BirA protein variants were prepared and purified as previously described,^{22,23} and the purity of each was estimated to be >95% based on Coomassie brilliant blue staining of samples subjected to sodium dodecyl sulfate–polyacrylamide gel electrophoresis. Protein concentrations were determined spectrophotometrically at 280 nm using a molar extinction coefficient of 47510 M^{−1} cm^{−1} calculated from the amino acid composition.²⁴ The fractional activity of each protein is >90% as determined by stoichiometric binding titrations with bio-S'-AMP monitored by steady-state fluorescence spectroscopy.²⁰

Sedimentation Equilibrium. The self-association of each BirA variant complexed with bio-S'-AMP was measured by equilibrium analytical ultracentrifugation using a Beckman Coulter Optima XL-I Analytical Ultracentrifuge. Proteins were first exchanged into SB:D₂O using Micro Bio-Spin 6 chromatography columns (Bio-Rad) as described by the manufacturer. For each measurement, protein prepared at three different concentrations was combined under stoichiometric conditions with bio-S'-AMP at a final molar ratio of 1:1.5. Equilibrium dissociation constants for binding of the ligand to the BirA variants range from picomolar to nanomolar.^{22,23} For each variant and/or solvent condition, the protein concentrations employed varied depending on the strength of the dimerization reaction. Lower concentrations were employed for tightly dimerizing systems and higher concentrations for weakly dimerizing systems, with the goal of optimizing representation of the dimer and monomer species in the concentration versus radial distance profiles. Samples were centrifuged in cells equipped with 12 mm six-hole or 3 mm two-hole charcoal-filled Epon centerpieces with quartz windows in a four-hole An-60 rotor (Beckman Coulter). Prior to centrifugation, the filled sample cells and rotor were incubated at the specified temperature for 1 h. Centrifugation was conducted at three rotor speeds ranging from 18000 to 24000 rpm. After the samples had reached equilibrium, scans were acquired with a step size of 0.001 cm with five averages at either 295 or 300 nm. At these wavelengths, the contribution from the absorbance of the adenosine moiety of bio-S'-AMP was avoided, and for samples prepared at very high protein concentrations, the total absorbance was in the linear range of the detection system.

Data Analysis. The absorbance versus radius profiles obtained for each scan were analyzed with WinNONLIN²⁵ using a single-species model to obtain σ , the reduced molecular weight, from which the weight-average molecular weight was calculated using the following equation:

$$\sigma = \frac{kM\left(1 - \frac{\bar{v}}{k}\rho\right)\omega^2}{RT} \quad (1)$$

where M is the molecular weight, k is the proportionality constant for the associated increase in the molecular weight and the decrease in the partial specific volume that occurs as a result of deuterium exchange into the protein,²⁶ \bar{v} is the protein partial specific volume, ρ is the buffer density, ω is the angular velocity of the rotor, R is the gas constant, and T is the temperature in kelvin. On the basis of a buffer composition of 95% (v/v) D₂O, a value for k of 1.0147 was used.²⁷ The partial specific volume of the BirA monomer is 0.755 mL/g,⁷ and the density was calculated from the buffer composition at the appropriate temperature using Sednterp (<http://sednterp.unh.edu/>).

Absorbance versus radius profiles were also globally analyzed to obtain the equilibrium association constant for dimerization, K_a , using the following monomer–dimer model:

$$C_t(r) = \delta + C_{\text{mon}}(r_0)e^{\frac{\sigma_{\text{mon}}}{2}\left(\frac{r^2}{r_0^2} - \frac{r_0^2}{r_0^2}\right)} + K_a[C_{\text{mon}}(r_0)]^2e^{\frac{2\sigma_{\text{mon}}}{2}\left(\frac{r^2}{r_0^2} - \frac{r_0^2}{r_0^2}\right)} \quad (2)$$

in which C_t is the total concentration at each radial position r , δ is the baseline offset, which was allowed to float in the analysis, and $C_{\text{mon}}(r_0)$ is the monomer concentration at reference radial position r_0 . For measurements performed at 20 °C, the σ_{mon} value used in calculations performed for wild-type and variant proteins is the measured value in D₂O buffer for wild-type apoBirA. In analysis of data acquired at other temperatures, the σ_{mon} value was adjusted for accompanying changes in the solvent density. In all analyses, the reduced molecular weight of the dimer was assumed to be twice that of the monomer. The quality of each fit was assessed from the magnitude of the square root of the variance and the distribution of the residuals of the fit about zero.

RESULTS

The HoloBirA Dimerization Reaction Is More Favorable in D₂O Than in H₂O. The equilibrium dimerization constant of wild-type holoBirA at 20 °C in standard buffer (10 mM Tris HCl, 200 mM KCl, and 2.5 mM MgCl₂) prepared with D₂O (SB:D₂O) was measured using sedimentation equilibrium. Initial analysis of the concentration versus radial position curves acquired at three loading concentrations and three speeds indicated weight-average molecular weights higher than that expected for the monomer (Figure 2). Global analysis

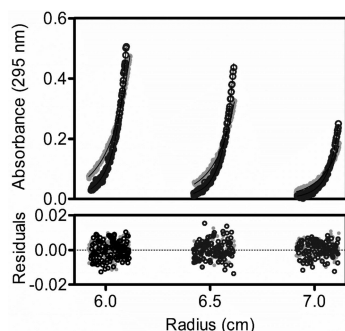


Figure 2. Sedimentation equilibrium measurements of wild-type holoBirA in SB:D₂O at 20 °C. HoloBirA prepared at 23, 15, and 7.5 μM (from left to right, respectively) was centrifuged at 18000 (gray circles) and 24000 rpm (empty circles). The lines correspond to the best-fit of nine data sets to a monomer–dimer model. For the sake of clarity, only six data sets are shown with the residuals of the fit.

using a monomer–dimer model yielded a best-fit equilibrium dissociation constant for dimerization of $(5 \pm 5) \times 10^{-7}$ M, indicating 12-fold tighter dimerization in SB:D₂O than in SB:H₂O (Table 1).

The Magnitude of the Effect of D₂O on HoloBirA Self-Association Is Conserved. The generality of the effect of D₂O on holoBirA self-association energetics was investigated by performing measurements on the single-alanine-substituted variants, T195A and V219A. These particular variants were chosen on the basis of the distinct locations of the substituted residues in the dimer structure and their altered dimerization energetics in H₂O relative to wild-type BirA. The T195 residue is located at the core of the dimer interface, and V219 is on the

dimer surface in a loop that folds over the adenylate moiety of bio-S'-AMP (Figure 3A). The equilibrium dissociation constants for dimerization of the T195A and V219A variants in SB:H₂O at 20 °C are 80 and 100 μM , respectively.^{22,23}

Sedimentation measurements for the bio-S'-AMP-bound forms of T195A and V219A in SB:D₂O were performed as described for wild-type BirA. The high affinities of both proteins for the ligand ensure that they are quantitatively in the holo form at the concentrations employed for the measurements. Global nonlinear least-squares analysis of the data yielded equilibrium dissociation constants for dimerization in D₂O buffer that are 10-fold smaller than those measured in H₂O buffer. Thus, similar to the effect observed for wild-type holoBirA dimerization, the Gibbs free energies calculated from the resolved equilibrium constants indicate -1.4 to -1.5 kcal/mol enhancements in dimerization of the variants resulting from the transfer of the reaction mixture from SB:H₂O to SB:D₂O (Figure 3B).

The Magnitude of the Coupling of Ligand, Bio-S'-AMP, Binding to BirA Dimerization Is Preserved in D₂O. BirA dimerization is thermodynamically coupled to bio-S'-AMP binding with a difference in dimerization free energy for the liganded, holoBirA, and unliganded, apoBirA, forms in SB:H₂O of -4 kcal/mol.⁸ The coupling in D₂O was investigated by performing sedimentation measurements on apoBirA prepared in SB:D₂O. In contrast to the holoBirA samples, which were prepared at low micromolar concentrations, the weak apoBirA dimerization necessitated measurements on samples prepared in the 100 μM concentration range. Global analysis of the data using a monomer–dimer model yielded an equilibrium dissociation constant of 600 μM , corresponding to a Gibbs free energy of -4.3 kcal/mol, -1.5 kcal more favorable than the value estimated for apoBirA in SB:H₂O.^{8,9} Calculation of the coupling free energy or $\Delta G^{\circ}_{\text{C,DIM}}$ from the dimerization free energies obtained for apo- and holoBirA in SB:D₂O yields a value of -4.2 ± 0.5 , identical, within error, to that obtained in SB:H₂O.

Enthalpic and Entropic Driving Forces for Dimerization in D₂O Differ Significantly from Those Measured in H₂O. In SB:H₂O at 20 °C, the modest holoBirA dimerization free energy results from large opposing enthalpic (ΔH°) and entropic ($-T\Delta S^{\circ}$) contributions of 41 and -48 kcal/mol, respectively.⁹ The solvent isotope effect on this thermodynamic signature was investigated by performing sedimentation measurements in SB:D₂O at temperatures ranging from 5 to 20 °C. The tight dimerization at higher temperatures precluded measurements above 20 °C. At each temperature, the data were acquired at three rotor speeds on samples prepared at three concentrations. At all temperatures, the data are described well by the monomer–dimer model and, as observed in SB:H₂O, the dimerization becomes tighter with an increase in temperature (Figure 4).⁹ The dimerization free energies calculated from the resolved equilibrium constants reveal that increasing the temperature from 5 to 20 °C renders the reaction more favorable by -1 kcal/mol. van't Hoff analysis of the data indicates a linear relationship (Figure 4) that yields a temperature-independent enthalpy, $\Delta H^{\circ}_{\text{DIM}}$, of 28 ± 3 kcal/mol. The entropic contributions to the dimerization free energy, calculated using the expression $\Delta G^{\circ}_{\text{DIM}} = \Delta H^{\circ} - T\Delta S^{\circ}$, are large and favorable over the entire temperature range (Figure 5). As observed in SB:H₂O, holoBirA dimerization in SB:D₂O is characterized by a large unfavorable enthalpy and a large favorable entropy. However, the absolute values of the

Table 1. Solvent Isotope Effects on BirA Dimerization

BirA variant	H ₂ O		D ₂ O		$\Delta\Delta G^{\circ}_{\text{Dim}}$ (kcal/mol) ^{b,c}
	K_{Dim} (M) ^a	$\Delta G^{\circ}_{\text{Dim}}$ (kcal/mol) ^b	K_{Dim} (M) ^a	$\Delta G^{\circ}_{\text{Dim}}$ (kcal/mol) ^b	
apo wild-type		(−2.8) ^d	$(6 \pm 1) \times 10^{-4}$	−4.3 ± 0.1	(−1.5) ^d
holo wild-type	$(6 \pm 2) \times 10^{-6}$	−7.0 ± 0.3	$(5 \pm 5) \times 10^{-7}$	−8.5 ± 0.5	−1.5 ± 0.6
V219A	$(8 \pm 1) \times 10^{-5}$	−5.5 ± 0.2	$(7 \pm 4) \times 10^{-6}$	−6.9 ± 0.3	−1.4 ± 0.4
T195A ^e	$(10 \pm 4) \times 10^{-5}$	−5.3 ± 0.2	$(9 \pm 7) \times 10^{-6}$	−6.8 ± 0.4	−1.5 ± 0.4

^aStandard errors reported are from two independent experiments. ^bStandard error propagation methods were used to determine the uncertainties for each reported value. ^c $\Delta\Delta G^{\circ}_{\text{Dim}} = \Delta G^{\circ}_{\text{Dim}}(\text{SB:D}_2\text{O}) - \Delta G^{\circ}_{\text{Dim}}(\text{SB:H}_2\text{O})$. ^dThe values provided for apoBirA were calculated using the equilibrium dissociation constant measured in SB:H₂O containing 50 mM KCl and assuming identical dependencies of apo- and holoBirA dimerization on KCl concentration.^{8,9} ^eThe equilibrium constant and Gibbs free energy of dimerization in H₂O for the T195A variant were previously reported.²³

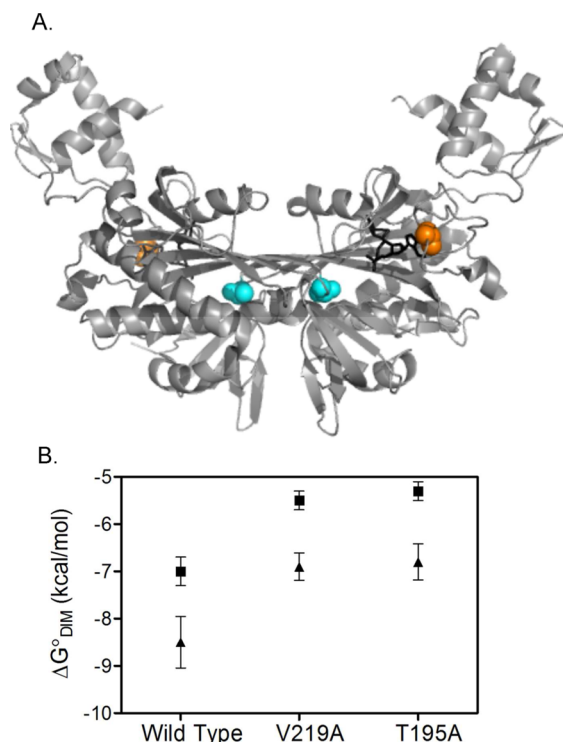


Figure 3. (A) Locations of alanine substitutions in the BirA structure. The T195A substitution (cyan) is at the dimerization interface, and the V219A substitution (orange) is in a loop that folds over the adenosine moiety and is on the outside surface of the dimer. The model was constructed in PyMol using Protein Data Bank entry 2EWN.^{12,44} (B) Energetic effects of the transfer of the dimerization reaction mixture from SB:H₂O to SB:D₂O. The Gibbs free energies of dimerization in H₂O (■) and D₂O (▲) indicate a consistent enhancement of −1.5 kcal/mol.

two energetic parameters in D₂O are markedly more modest than in H₂O.

DISCUSSION

BirA Dimerization Is Enhanced in D₂O Relative to That in H₂O. HoloBirA self-association in D₂O is energetically more favorable than in H₂O. Sedimentation equilibrium measurements of wild-type holoBirA dimerization indicate a 12-fold decrease in the equilibrium dissociation constant in D₂O relative to that in H₂O, corresponding to a −1.5 kcal/mol enhancement in the dimerization free energy. Measurements performed on two BirA variants with single-alanine substitutions as well as apoBirA indicate enhancements of identical magnitude. The distinct locations of the two substitutions in

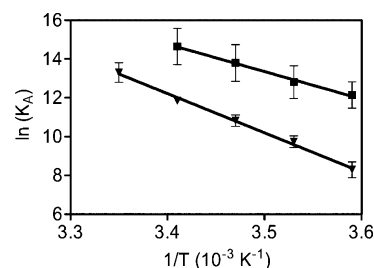


Figure 4. van't Hoff analysis of the temperature dependence of the equilibrium constant for holoBirA dimerization in SB:D₂O (■) and SB:H₂O (▼). The lines correspond to the best fits of the data to the van't Hoff equation. The data obtained in SB:H₂O were taken from ref 9.

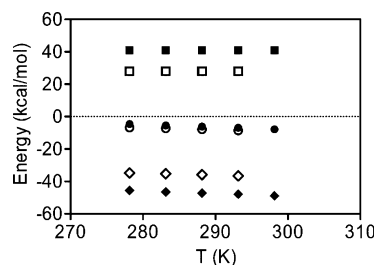


Figure 5. Thermodynamic signatures for holoBirA dimerization in SB:H₂O and SB:D₂O. The energetic terms in H₂O and D₂O are $\Delta G^{\circ}_{\text{Dim}}$ (● and ○), $\Delta H^{\circ}_{\text{Dim}}$ (■ and □), and $-T\Delta S^{\circ}_{\text{Dim}}$ (◆ and ◇). The values in SB:H₂O were taken from ref 9. On the scale used for the graph, the estimated errors in the values are within the symbols.

the three-dimensional structure of BirA underscore the general effect of D₂O on the reaction. The T195A substitution is located in a loop in the dimerization interface. By contrast, the V219A substitution is in a surface loop that folds over the adenylate moiety of the ligand bio-5'-AMP, 24 Å from the interface.¹²

Although holoBirA dimerization in D₂O is enhanced relative to the reaction in H₂O, no effect on the linkage between corepressor binding and dimerization is observed. Bio-5'-AMP enhances BirA dimerization in both H₂O and D₂O with a coupling free energy of −4.0 kcal/mol, a result consistent with the general effect of the heavier solvent on dimerization. However, the coupling free energy in H₂O was determined in buffer containing 50 mM KCl rather than the 200 mM KCl used in the studies presented here.⁸ Thus, the conclusion that coupling free energies are equivalent in the two solvents assumes no influence of salt concentration on coupling. The measured modest effect of monovalent salt concentration on holoBirA dimerization supports this assumption.⁹

Previous studies indicate increases in the level of self-association in D₂O relative to H₂O for several proteins, including phycocyanin,²⁸ glutamate dehydrogenase,²⁹ and α -chymotrypsin.³⁰ For the limited number of studies that provided quantitative information, the magnitude of the effect varies. For example, at 4 °C self-association of tobacco mosaic virus coat protein is modestly enhanced by 3-fold in D₂O versus H₂O.³¹ A 10-fold enhancement of β -lactoglobulin A self-association is observed in heavy water, similar in magnitude to the effect on BirA dimerization.³²

The Thermodynamics in H₂O and D₂O Are Consistent with Coupling of Solvent Release to HoloBirA Dimerization. The measurements of holoBirA dimerization as a function of temperature in heavy water provide additional support for a significant contribution of solvent release to the energetics of the process. The dimerization enthalpies obtained in SB:H₂O and SB:D₂O are 41 ± 3 and 28 ± 3 kcal/mol, respectively. At 20 °C, the entropic contributions, $-T\Delta S^\circ$, to dimerization free energy are -48 and -36 kcal/mol, respectively, in the two buffers. As observed in H₂O, the net modest dimerization free energy of -8.5 kcal/mol in D₂O reflects large opposing enthalpies and entropies, albeit significantly more modest than those obtained in H₂O. These differences in the dimerization thermodynamics exist over the temperature range employed for the measurements (Figure 5). In both solvents, the net unfavorable dimerization enthalpy reflects the penalty of desolvating the polar dimerization surface. However, this removal is energetically offset, in part, by formation of intersolvent hydrogen bonds that accompanies its release to the bulk. The more modest unfavorable enthalpy measured for the reaction in D₂O than in H₂O reflects the stronger bonding between the heavy water molecules.³³ Likewise, this stronger bonding yields a less favorable dimerization entropy in D₂O than in H₂O.³³ The very slow holoBirA dimerization kinetics estimated from analysis of sedimentation velocity data provides additional support for a significant role of solvent release in the process.³⁴ Simulations of protein aggregation indicate a high kinetic barrier to solvent release from polar side chains.³⁵ The favorable interaction of water with the charged and polar residues on the BirA dimerization surface should result in a similarly high barrier to dimer formation.

The solvent isotope effect on holoBirA dimerization thermodynamics is significantly larger than that measured for other protein association reactions. For example, measurements of the dimer–octamer equilibrium of β -lactoglobulinA yielded enthalpies of -64 and -69 kcal/mol in H₂O and D₂O, respectively.³² Indeed, solvent isotope effects of the magnitude observed in this work have been reported only for protein folding,³⁶ which may indicate a more significant role for solvent release in the holoBirA dimerization reaction than for other protein association reactions. Solvent isotope effects on protein folding and association reactions have previously been ascribed to stronger bonding resulting from exchange of deuterium for hydrogen in hydrogen bonding partners.^{33,37} Alternatively, the decreased flexibility observed for some proteins in D₂O may alter interaction thermodynamics.^{38,39} For BirA, the absence of a solvent isotope effect on coupling between adenylate binding and dimerization points to solvent release being the major source of the distinct thermodynamic profiles measured in the two solvents.

Practical Implications for Hydrogen–Deuterium Exchange Studies. Hydrogen–deuterium exchange measurements, detected by either mass spectrometry or nuclear

magnetic resonance spectroscopy, are used to study protein folding, dynamics, and interactions.^{40,41} The potential for solvent isotope perturbation of protein function has previously been suggested.^{42,43} Results reported in this work, which indicate that these effects can be large in magnitude, underscore the importance of performing appropriate controls to determine the functional effects of transferring a biomolecular system from H₂O to D₂O.

AUTHOR INFORMATION

Corresponding Author

*E-mail: dbeckett@umd.edu. Phone: (301) 405-1812.

Funding

This work was supported in part by National Institutes of Health Grants R01GM46511 and S10RR15899 to D.B.

Notes

The authors declare no competing financial interest.

ABBREVIATIONS

BirA, *E. coli* bifunctional biotin repressor/biotin protein ligase; holoBirA, BirA bound to bio-5'-AMP; apoBirA, ligand free BirA; bio-5'-AMP, biotinoyl-5'-adenosine monophosphate; Tris, tris(hydroxymethyl)aminomethane; SB, standard buffer [10 mM Tris, 200 mM KCl, and 2.5 mM MgCl₂ (pH 7.5) at the working temperature]; SB:H₂O, standard buffer prepared in H₂O; SB:D₂O, standard buffer prepared in D₂O.

REFERENCES

- (1) Hodkinson, P. S., Elliott, P. A., Lad, Y., McHugh, B. J., MacKinnon, A. C., Haslett, C., and Sethi, T. (2007) Mammalian NOTCH-1 activates β 1 integrins via the small GTPase R-Ras. *J. Biol. Chem.* 282, 28991–29001.
- (2) Layer, J. H., Miller, S. G., and Weil, P. A. (2010) Direct transactivator-transcription factor IID (TFIID) contacts drive yeast ribosomal protein gene transcription. *J. Biol. Chem.* 285, 15489–15499.
- (3) Dickinson, D. J., Robinson, D. N., Nelson, W. J., and Weis, W. I. (2012) α -Catenin and IQGAP regulate myosin localization to control epithelial tube morphogenesis in *Dictyostelium*. *Dev. Cell* 23, 533–546.
- (4) Thirumalai, D., Reddy, G., and Straub, J. E. (2012) Role of water in protein aggregation and amyloid polymorphism. *Acc. Chem. Res.* 45, 83–92.
- (5) Stranges, P. B., and Kuhlman, B. (2013) A comparison of successful and failed protein interface designs highlights the challenges of designing buried hydrogen bonds. *Protein Sci.* 22, 74–82.
- (6) Streaker, E. D., and Beckett, D. (2003) Coupling of protein assembly and DNA binding: Biotin repressor dimerization precedes biotin operator binding. *J. Mol. Biol.* 325, 937–948.
- (7) Eisenstein, E., and Beckett, D. (1999) Dimerization of the *Escherichia coli* biotin repressor: corepressor function in protein assembly. *Biochemistry* 38, 13077–13084.
- (8) Streaker, E. D., Gupta, A., and Beckett, D. (2002) The biotin repressor: Thermodynamic coupling of corepressor binding, protein assembly, and sequence-specific DNA binding. *Biochemistry* 41, 14263–14271.
- (9) Zhao, H., Streaker, E., Pan, W., and Beckett, D. (2007) Protein-protein interactions dominate the assembly thermodynamics of a transcription repression complex. *Biochemistry* 46, 13667–13676.
- (10) Khalil, M. T., and Lauffer, M. A. (1967) Polymerization-depolymerization of tobacco mosaic virus protein. X. Effect of D₂O. *Biochemistry* 6, 2474–2480.
- (11) Baldwin, R. L. (2010) Desolvation penalty for burying hydrogen-bonded peptide groups in protein folding. *J. Phys. Chem. B* 114, 16223–16227.
- (12) Wood, Z., Weaver, L. H., Brown, P. H., Beckett, D., and Matthews, B. W. (2006) Co-repressor induced order and biotin

repressor dimerization: A case for divergent followed by convergent evolution. *J. Mol. Biol.* 357, 509–523.

(13) Saha, R. P., Bahadur, R. P., Pal, A., Mandal, S., and Chakrabarti, P. (2006) ProFace: A server for the analysis of the physicochemical features of protein-protein interfaces. *BMC Struct. Biol.* 6, 11.

(14) Krissinel, E., and Henrick, K. (2007) Inference of macromolecular assemblies from crystalline state. *J. Mol. Biol.* 372, 774–797.

(15) Courtenay, E. S., Capp, M. W., Anderson, C. F., and Record, M. T., Jr. (2000) Vapor pressure osmometry studies of osmolyte-protein interactions: Implications for the action of osmoprotectants in vivo and for the interpretation of “osmotic stress” experiments in vitro. *Biochemistry* 39, 4455–4471.

(16) Kornblatt, M. J., Kornblatt, J. A., and Hui Bon Hoa, G. (1993) The role of water in the dissociation of enolase, a dimeric enzyme. *Arch. Biochem. Biophys.* 306, 495–500.

(17) Zhai, Y., Okoro, L., Cooper, A., and Winter, R. (2011) Applications of pressure perturbation calorimetry in biophysical studies. *Biophys. Chem.* 156, 13–23.

(18) Chervenak, M. C., and Toone, E. J. (1994) A Direct Measure of the Contribution of Solvent Reorganization to the Enthalpy of Ligand-Binding. *J. Am. Chem. Soc.* 116, 10533–10539.

(19) Lane, M. D., Rominger, K. L., Young, D. L., and Lynen, F. (1964) The enzymatic synthesis of holotranscarboxylase from apotranscarboxylase and (+)-biotin. *J. Biol. Chem.* 239, 2865–2871.

(20) Abbott, J., and Beckett, D. (1993) Cooperative binding of the *Escherichia coli* repressor of biotin biosynthesis to the biotin operator sequence. *Biochemistry* 32, 9649–9656.

(21) Glasoe, P. K., and Long, F. A. (1960) Use of Glass Electrodes to Measure Acidities in Deuterium Oxide. *J. Phys. Chem.* 64, 188–190.

(22) Naganathan, S., and Beckett, D. (2007) Nucleation of an allosteric response via ligand-induced loop folding. *J. Mol. Biol.* 373, 96–111.

(23) Adikaram, P. R., and Beckett, D. (2012) Functional versatility of a single protein surface in two protein:protein interactions. *J. Mol. Biol.* 419, 223–233.

(24) Gill, S. C., and von Hippel, P. H. (1989) Calculation of protein extinction coefficients from amino acid sequence data. *Anal. Biochem.* 182, 319–326.

(25) Johnson, M. L., Correia, J. J., Yphantis, D. A., and Halvorson, H. R. (1981) Analysis of data from the analytical ultracentrifuge by nonlinear least-squares techniques. *Biophys. J.* 36, 575–588.

(26) Martin, W. G., Winkler, C. A., and Cook, W. H. (1959) Partial Specific Volume Measurements by Differential Sedimentation. *Can. J. Chem.* 37, 1662–1670.

(27) Edelstein, S. J., and Schachman, H. K. (1967) The simultaneous determination of partial specific volumes and molecular weights with microgram quantities. *J. Biol. Chem.* 242, 306–311.

(28) Lee, J. J., and Berns, D. S. (1968) Protein aggregation. The effect of deuterium oxide on large protein aggregates of C-phycocyanin. *Biochem. J.* 110, 465–470.

(29) Woodfin, B. M., Henderson, R. F., and Henderson, T. R. (1970) Effects of D₂O on the association-dissociation equilibrium in subunit proteins. *J. Biol. Chem.* 245, 3733–3737.

(30) Aune, K. C., Goldsmith, L. C., and Timasheff, S. N. (1971) Dimerization of α -chymotrypsin. II. Ionic strength and temperature dependence. *Biochemistry* 10, 1617–1622.

(31) Paglini, S., and Lauffer, M. A. (1968) Polymerization-depolymerization of tobacco mosaic virus protein. XI. Osmotic pressure studies of solutions in water and in deuterium. *Biochemistry* 7, 1827–1835.

(32) Baghurst, P. A., Nichol, L. W., and Sawyer, W. H. (1972) The effect of D₂O on the association of α -lactoglobulin A. *J. Biol. Chem.* 247, 3199–3204.

(33) Nemethy, G., and Scheraga, H. A. (1964) Structure of Water + Hydrophobic Bonding in Proteins. 4. Thermodynamic Properties of Liquid Deuterium Oxide. *J. Chem. Phys.* 41, 680.

(34) Zhao, H., and Beckett, D. (2008) Kinetic partitioning between alternative protein-protein interactions controls a transcriptional switch. *J. Mol. Biol.* 380, 223–236.

(35) Reddy, G., Straub, J. E., and Thirumalai, D. (2010) Dry amyloid fibril assembly in a yeast prion peptide is mediated by long-lived structures containing water wires. *Proc. Natl. Acad. Sci. U.S.A.* 107, 21459–21464.

(36) Makhatadze, G. I., Clore, G. M., and Gronenborn, A. M. (1995) Solvent isotope effect and protein stability. *Nat. Struct. Biol.* 2, 852–855.

(37) Cho, Y., Sagle, L. B., Iimura, S., Zhang, Y., Kherb, J., Chilkoti, A., Scholtz, J. M., and Cremer, P. S. (2009) Hydrogen bonding of β -turn structure is stabilized in D₂O. *J. Am. Chem. Soc.* 131, 15188–15193.

(38) Cioni, P., and Strambini, G. B. (2002) Effect of heavy water on protein flexibility. *Biophys. J.* 82, 3246–3253.

(39) Tehei, M., Madern, D., Pfister, C., and Zaccai, G. (2001) Fast dynamics of halophilic malate dehydrogenase and BSA measured by neutron scattering under various solvent conditions influencing protein stability. *Proc. Natl. Acad. Sci. U.S.A.* 98, 14356–14361.

(40) Konermann, L., Pan, J., and Liu, Y. H. (2011) Hydrogen exchange mass spectrometry for studying protein structure and dynamics. *Chem. Soc. Rev.* 40, 1224–1234.

(41) Lee, Y. H., and Goto, Y. (2012) Kinetic intermediates of amyloid fibrillation studied by hydrogen exchange methods with nuclear magnetic resonance. *Biochim. Biophys. Acta* 1824, 1307–1323.

(42) Sackett, D. L., Chernomordik, V., Krueger, S., and Nossal, R. (2003) Use of small-angle neutron scattering to study tubulin polymers. *Biomacromolecules* 4, 461–467.

(43) Prasanna, C. B., Artigues, A., and Fenton, A. W. (2011) Monitoring allostery in D₂O: A necessary control in studies using hydrogen/deuterium exchange to characterize allosteric regulation. *Anal. Bioanal. Chem.* 401, 1083–1086.

(44) DeLano, W. L. (2002) *The PyMOL Molecular Graphics System*, version 1.2r3pre, Schrödinger, LLC, Portland, OR.